Inorg. Chem. **2005**, *44*, 1955–1965

Intramolecular Metal···Sulfur Interactions of Platinum(II) 1,4,7-Trithiacyclononane Complexes with Bipyridyl Ligands: The Relationship between Molecular and Electronic Structures

Tyler W. Green, Rachel Lieberman, Neal Mitchell, Jeanette A. Krause Bauer, and William B. Connick*

Department of Chemistry, University of Cincinnati, P.O. Box 210172, Cincinnati, Ohio 45221-0172

Received October 6, 2004

Five platinum(II) 1,4,7-trithiacyclononane (ttcn) complexes with bidentate-substituted 2,2′-bipyridine ligands have been prepared and structurally characterized: $[Pt(bpy)(ttcn)](PF_6)_2$ (bpy = 2,2′-bipyridine), triclinic, $P\bar{1}$, $a = 10.2529(3)$ Å, $b = 10.7791(3)$ Å, $c = 10.7867(3)$ Å, $\alpha = 83.886(1)°$, $\beta = 87.565(1)°$, $\gamma = 84.901(1)$, $V = 1179.99(6)$ Å^3, $Z = 2$; $[Pt(4,4'\text{-dmbpy})(ttcn)](PF_6)_2 \cdot CH_3CN \cdot H_2O$ (4,4′-dmbpy = 4,4′-dimethyl-2,2′-bipyridine), triclinic, $P\bar{1}$, $a = 10.1895(3)$ Å, $b = 11.8566(4)$ Å, $c = 13.1004(4)$ Å, $\alpha = 77.345(1)°$, $\beta = 79.967(1)°$, $\gamma = 72.341(1)°$, $V = 1461.56(8)$ Å^3, $Z = 2$; $[Pt(5,5'\text{-dmbpy})(ttcn)](PF_6)_2$ (5,5′-dmbpy = 5,5′-dimethyl-2,2′-bipyridine), triclinic, $P\bar{1}$, $a = 10.6397(4)$ Å, $b = 10.8449(4)$ Å, $c = 11.2621(4)$ Å, $\alpha = 90.035(1)°$, $\beta = 98.061(1)°$, $\gamma = 91.283(1)°$, $V = 1286.32(8)$ Å^3, $Z = 2$; $[Pt(dbbpy)(ttcn)](PF_6)_2 \cdot CH_3NO_2$ (dbbpy = 4,4′-di-*tert*-butyl-2,2′-bipyridine), triclinic, $P\bar{1}$, $a = 11.5422(7)$ Å, $b = 11.6100(7)$ Å, $c = 13.6052(9)$ Å, $\alpha = 85.902(1)°$, $\beta = 89.675(1)°$, $\gamma = 74.942(1)°$, $V = 1755.90(19)$ Å^3, $Z = 2$; and $[Pt(dtfmbpy)(ttcn)](PF_6)_2 \cdot CH_3CN$ (dtfmbpy = 5,5′-di-trifluoromethyl-2,2′-bipyridine): monoclinic, $P2_1/c$, $a = 13.1187(9)$ Å, $b = 20.9031(15)$ Å, $c = 11.3815(8)$ Å, $\beta = 105.789(2)°$, $V = 3003.3(4)$ Å^3, $Z = 4$. For each salt, the platinum(II) center of the cation is bonded to two nitrogen atoms of the chelating diimine and two sulfur atoms of the thioether macrocycle. The third sulfur atom of ttcn forms a long apical interaction with the metal center (2.84–2.97 Å), resulting in a flattened square pyramid structure. An examination of these and 17 other structures of platinum(II) ttcn complexes reveals a correlation between the apical Pt···S distance and the donor properties of the ancillary ligands, suggesting a means for using variations in ligand electronic properties to tune molecular structure. The room-temperature absorption spectra in acetonitrile solution show a broad and comparatively low-energy MLCT band maximizing near ~390 nm for the bpy and dialkyl-substituted bipyridyl derivatives. The maximum is dramatically red-shifted to 460 nm in the spectrum of the dtfmbpy complex as a result of the electron-withdrawing properties of the $-CF_3$ groups. The 3:1 EtOH/MeOH 77 K glassy solution emission spectra exhibit low-energy emission bands (λ_{max}, 570–645 nm), tentatively assigned as originating from a lowest, predominantly spin-forbidden MLCT excited state that is stabilized by apical Pt···S interactions.

Introduction

Intramolecular interactions of a dangling nucleophile with a platinum(II) center at the vacant axial sites of a square planar complex can have a profound influence on dynamics and reactivity, and investigations of these effects are providing insight into ligand exchange reactions and multi-redox catalysis.[1,2] We have recently proposed that preorganization of one or both of the pendant amine groups around the metal center of $Pt(pip_2NCN)(tpy)^+$ plays a critical role in this compound's remarkable outer-sphere two-electron reactivity.[3]

To better gauge the influence of axial interactions on the electronic structures of platinum(II) complexes with polypyridyl ligands, we have undertaken an investigation of the structures and spectroscopic properties of a series of platinum(II) 1,4,7-trithiacyclononane (ttcn) complexes with bidentate-substituted 2,2′-bipyridine ligands. Nikol et al.[2] previously have shown that two of the ttcn sulfur atoms of $[Pt(phen)(ttcn)](PF_6)_2$ (phen = 1,10-phenanthroline) form short Pt−S bonds (2.272(3), 2.279(3) Å), whereas the third

* Author to whom correspondence should be addressed. E-mail: bill.connick@uc.edu.

10.1021/ic048610d CCC: $30.25
Published on Web 02/19/2005

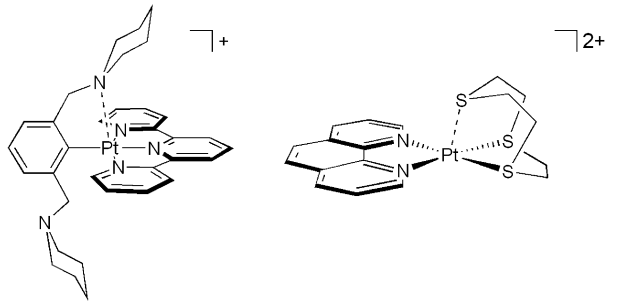

$Pt(pip_2NCN)(tpy)^+$ $Pt(phen)(ttcn)^{2+}$

sulfur adopts a somewhat longer Pt···S distance (2.821(3) Å). Similar distorted square pyramid structures have been reported for platinum(II) ttcn complexes with ancillary phosphine and halide ligands, although the apical Pt···S distances vary widely (2.64−3.26 Å).[4−13] Given these observations and that platinum(II) bipyridyl complexes exhibit rich electronic spectroscopy,[14] the targeted systems are ripe for investigations of the delicate interplay between molecular and electronic structures. Here, we present evidence suggesting that the electronic properties of the ancillary ligands influence the apical Pt···S interactions of platinum(II) ttcn systems. In addition, we find that these interactions persist to a significant extent in solutions and strongly influence the absorption and emission properties of complexes with bipyridyl ligands. The accumulated data suggest guidelines for exploiting the intimate relationship between molecular and electronic structures to control preorganization and reactivity of this general class of compounds.

Experimental Section

K_2PtCl_4 was obtained from Pressure Chemical (Pittsburgh, PA). 1,4,7-Trithiacyclononane (ttcn) was obtained from Aldrich Chemical Co. (Milwaukee, WI). All other reagents were obtained from Acros (Somerville, NJ). Acetonitrile for UV−visible absorption and electrochemical studies was distilled from calcium hydride. Ethanol for emission studies was distilled under argon from zinc and potassium hydroxide. All other chemicals were used as received. 5,5′-Di-trifluoromethyl-2,2′-bipyridine (dtfmbpy) was prepared according to the literature procedure.[15] $Pt(bpy)Cl_2$ was prepared by the method of Morgan and Burstall,[16] and $Pt(4,4'\text{-dmbpy})Cl_2$, $Pt(5,5'\text{-dmbpy})Cl_2$, $Pt(dbbpy)Cl_2$, and $Pt(dtfmbpy)Cl_2$ were prepared in a similar manner. $[Pt(bpy)(1,4\text{-dithn})](PF_6)_2$ (1,4-dithn=1,4-dithiane) was prepared by modification of the literature procedure.[17] Elemental analyses were performed by Atlantic Microlab, Inc. (Norcross, GA). ^{1}H NMR spectra were recorded at room temperature using a Bruker AC 250 MHz instrument. Deuterated acetonitrile and acetone were obtained from Cambridge Isotope Laboratories (Andover, MA). All ^{1}H NMR spectra are referenced in ppm with respect to a TMS standard. Mass spectra were obtained by electrospray ionization of acetonitrile solutions using either an Ionspec HiRes ESI-FTICRMS instrument or a Micromass Q-TOF-II instrument. UV−visible absorption spectra were recorded using a HP8453 Diode Array spectrometer. Electrochemical measurements were recorded using a standard three-electrode cell and a CV50w potentiostat or 100 B/W electrochemical workstation from Bioanalytical Systems. Scans were recorded in distilled acetonitrile solution containing 0.1 M tetrabutylammonium hexafluorophosphate ($TBAPF_6$), which was recrystallized at least twice from methanol and dried under vacuum prior to use. All scans were recorded using a Pt wire auxiliary electrode, a Ag/AgCl (3.0 M NaCl) reference electrode, and a 0.79 mm^2 Au working electrode. Reported potentials are referenced vs Ag/AgCl (3.0 M NaCl). Emission spectra were recorded using a SPEX Fluorolog-3 fluorimeter equipped with a double emission monochromator and a single excitation monochromator. 77 K glassy solutions were prepared by inserting a quartz EPR tube containing a 4:1 EtOH:MeOH solution of the complex into a quartz-tipped finger dewar. Emission spectra were corrected for instrumental response.

$[Pt(bpy)(ttcn)](PF_6)_2$. $Pt(bpy)Cl_2$ (0.309 g, 0.73 mmol) and slightly less than 1 equiv of ttcn (0.127 g, 0.71 mmol) were refluxed in a 1:1:1 mixture of distilled water, methanol, and acetonitrile (300 mL) for 3 h under argon. After the mixture was cooled to room temperature, excess NH_4PF_6 was added to the resulting red solution. Approximately two-thirds of the solvent was removed, and red crystals of the product formed upon cooling to 0 °C. The product was washed with diethyl ether and cold ethanol before being dried in vacuo. Yield 0.548 g, 91.2%. Orange crystals of the product

(1) For example: (a) Blake, A. J.; Gould, R. O.; Holder, A. J.; Hyde, T. I.; Lavery, A. J.; Odulate, M. O.; Schröder, M. *J. Chem. Soc., Dalton Trans.* **1987**, 118−120. (b) Blake, A. J.; Crofts, R. D.; Schröder, M. *J. Chem. Soc., Dalton Trans.* **1993**, 2259−2260. (c) Grant, G. J.; Spangler, N. J.; Setzer, W. N.; VanDerveer, D. G.; Mehne, L. F. *Inorg. Chim. Acta* **1996**, *246*, 31−40. (d) Matsumoto, M.; Funahashi, S.; Takagi, H. D. *Z. Naturforsch.* **1999**, *54B*, 1138−1146. (e) Mitsuru, M.; Itoh, M.; Funahashi, S.; Takagi, H. D. *Can. J. Chem.* **1999**, *77*, 1638−1647. (f) Wieghardt, K.; Koeppen, M.; Swiridoff, W.; Weiss, J. *J. Chem. Soc., Dalton Trans.* **1983**, 1869−1872. (g) Norris, C. M.; Reinartz, S.; White, P. S.; Templeton, J. L. *Organometallics* **2002**, *21*, 5649−5656. (h) Jensen, M. P.; Wick, D. D.; Reinartz, S.; White, P. S.; Templeton, J. L.; Goldberg, K. I. *J. Am. Chem. Soc.* **2003**, *125*, 8614−8624. (i) Wick, D. D.; Goldberg, K. I. *J. Am. Chem. Soc.* **1997**, *119*, 10235−10236. (j) Haskel, A.; Keinan, E. *Organometallics* **1999**, *18*, 4677−4680. (k) Reinartz, S.; White, P. S.; Brookhart, M.; Templeton, J. L. *Organometallics* **2000**, *19*, 3854−3866. (l) Haines, R. I.; Hutchings, D. R.; McCormack, T. M. *J. Inorg. Biochem.* **2001**, *85*, 1−7. (m) Hinman, J. G.; Baar, C. R.; Jennings, M. C.; Puddephatt, R. J. *Organometallics* **2000**, *19*, 563−570. (n) Faissner, R.; Huttner, G.; Kaifer, E.; Kircher, P.; Rutsch, P.; Zsolnai, L. *Eur. J. Inorg. Chem.* **2003**, 2219−2238.
(2) Nikol, H.; Bürgi, H.-B.; Hardcastle, K. I.; Gray, H. B. *Inorg. Chem.* **1995**, *34*, 6319−6322.
(3) Jude, H.; Krause Bauer, J. A.; Connick, W. B. *J. Am. Chem. Soc.* **2003**, *125*, 3446−3447.
(4) Grant, G. J.; Poullaos, I. M.; Galas, D. F.; VanDerveer, D. G.; Zubkowski, J. D.; Valente, E. J. *Inorg. Chem.* **2001**, *40*, 564−567.
(5) Grant, G. J.; Pool, J. A.; VanDerveer, D. G. *J. Chem. Soc., Dalton Trans.* **2003**, 3981−3984.
(6) Grant, G. J.; Galas, D. F.; Carter, S. M.; VanDerveer, D. G. *J. Chem. Soc., Dalton Trans.* **2002**, 2973−2980.
(7) Grant, G. J.; Galas, D. F.; VanDerveer, D. G. *Polyhedron* **2002**, *21*, 879−884.
(8) Grant, G. J.; Brandow, C. G.; Galas, D. F.; Davis, J. P.; Pennington, W. T.; Valente, E. J.; Zubkowski, J. D. *Polyhedron* **2001**, *20*, 3333−3342.
(9) Grant, G. J.; Carter, S. M.; Russell, A. L.; Poullaos, I. M.; VanDerveer, D. G. *J. Organomet. Chem.* **2001**, *637−639*, 683−690.
(10) Bennett, M. A.; Canty, A. J.; Felixberger, J. K.; Rendina, L. M.; Sunderland, C.; Willis, A. C. *Inorg. Chem.* **1993**, *32*, 1951−1958.
(11) Bennett, M. A.; Felixberger, J. K.; Willis, A. C. *Gazz. Chim. Ital.* **1993**, *123*, 405−408.
(12) Blake, A. J.; Gould, R. O.; Holder, A. J.; Hyde, T. I.; Lavery, A. J.; Odulate, M. O.; Schröder, M. *J. Chem. Soc., Chem. Commun.* **1987**, 118−120.
(13) Contu, F.; Demartin, F.; Devillanova, F. A.; Garau, A.; Isaia, F.; Lippolis, V.; Salis, A.; Verani, G. *J. Chem. Soc., Dalton Trans.* **1997**, 4401−4405.
(14) For a recent review, see: Fleeman, W. D.; Connick, W. B. *Comments Inorg. Chem.* **2002**, *23*, 205−230.
(15) Chan, K. S.; Tse, A. K.-S. *Synth. Commun.* **1993**, *23*, 1929−1934.
(16) Morgan, G. T.; Burstall, F. H. *J. Chem. Soc.* **1934**, 965−971.
(17) Tierney, E. J.; Sabatelli, A. D.; Sarneski, J. E. *Inorg. Chem.* **1987**, *26*, 617−620.

were grown by slow diffusion of diethyl ether into an acetonitrile solution. Anal. Calcd for $PtC_{16}H_{20}N_2S_3P_2F_{12}$: C, 23.39; H, 2.45; N, 3.41. Found: C, 23.61; H, 2.37; N, 3.48. MS-ESI (*m*/*z*): 676.0 ([Pt(bpy)(ttcn)]$(PF_6)^+$), 265.5 ([Pt(bpy)(ttcn)]$^{2+}$). ^{1}H NMR (CD_3CN, δ): 8.88 (2H, d with Pt satellites, $J_{H-Pt} = 36$ Hz, 6,6′-H), 8.52−8.44 (4H, m, 3,3′-H and 4,4′-H), 7.81 (2H, dd, 5,5′-H), 3.30−3.05 (12H, m, ttcn).

[Pt(4,4′-dmbpy)(ttcn)](PF$_6$)$_2$. The product was isolated as a yellow crystalline material by following the procedure for [Pt(bpy)(ttcn)]$(PF_6)_2$ and substituting Pt(4,4′-dmbpy)Cl_2 (0.228 g, 0.51 mmol) for Pt(bpy)Cl_2. Yield 0.408 g, 91.5%. Anal. Calcd for $PtC_{18}H_{24}N_2S_3P_2F_{12}$: C, 25.45; H, 2.85; N, 3.30. Found: C, 25.73; H, 2.82; N, 3.50. MS-ESI (*m*/*z*): 704.0 ([Pt(4,4′-dmbpy)(ttcn)]$(PF_6)^+$), 279.5 ([Pt(4,4′-dmbpy)(ttcn)]$^{2+}$). ^{1}H NMR (CD_3CN, δ): 8.67 (2H, d with Pt satellites, $J_{H-Pt} = 35$ Hz, 6,6′-H), 8.34 (2H, s, 3,3′-H), 7.62 (2H, d, 5,5′-H), 3.25−3.07 (12H, m, ttcn), 2.62 (6H, s, CH_3).

[Pt(5,5′-dmbpy)(ttcn)](PF$_6$)$_2$. The product was isolated as an orange crystalline material by following the procedure for [Pt(bpy)(ttcn)]$(PF_6)_2$ and substituting Pt(5,5′-dmbpy)Cl_2 (0.395 g, 0.88 mmol) for Pt(bpy)Cl_2. Yield 0.647 g, 87.9%. Anal. Calcd for $PtC_{18}H_{24}N_2S_3P_2F_{12}$: C, 25.45; H, 2.85; N, 3.30. Found: C, 25.47; H, 2.76; N, 3.34. MS-ESI (*m*/*z*): 704.0 ([Pt(5,5′-dmbpy)(ttcn)]$(PF_6)^+$), 279.5 ([Pt(5,5′-dmbpy)(ttcn)]$^{2+}$). ^{1}H NMR (CD_3CN, δ): 8.60 (2H, s with Pt satellites, $J_{H-Pt} = 36$ Hz, 6,6′-H), 8.33−8.21 (4H, m, 3,3′-H and 4,4′-H), 3.31−3.04 (12H, m, ttcn), 2.53 (6H, s, CH_3).

[Pt(dbbpy)(ttcn)](PF$_6$)$_2$. The product was isolated as a yellow-orange crystalline material by following the procedure for [Pt(bpy)(ttcn)]$(PF_6)_2$ and substituting Pt(dbbpy)Cl_2 (0.539 g, 1.01 mmol) for Pt(bpy)Cl_2. Yield 0.504 g, 53.5%. Anal. Calcd for $PtC_{24}H_{36}N_2S_3P_2F_{12}$: C, 30.87; H, 3.89; N, 3.00. Found: C, 31.15; H, 3.85; N, 3.09. MS-ESI (*m*/*z*): 788.1 ([Pt(dbbpy)(ttcn)]$(PF_6)^+$), 321.6 ([Pt(dbbpy)(ttcn)]$^{2+}$). ^{1}H NMR (CD_3CN, δ): 8.73 (2H, d with Pt satellites, $J_{H-Pt} = 35$ Hz, 6,6′-H), 8.45 (2H, s, 3,3′-H), 7.76 (2H, d, 5,5′-H), 3.29−3.05 (12H, m, ttcn), 1.47 (18H, s, *t*-Bu).

[Pt(dtfmbpy)(ttcn](PF$_6$)$_2$. The product was isolated as a red crystalline material by following the procedure for [Pt(bpy)(ttcn)]$(PF_6)_2$ and substituting Pt(dtfmbpy)Cl_2 (0.100 g, 0.18 mmol) for Pt(bpy)Cl_2. Yield 0.136 g, 79.1%. Anal. Calcd for $PtC_{18}H_{18}N_2S_3P_2F_{18}$: C, 22.58; H, 1.89; N, 2.93. Found: C, 22.74; H, 2.02; N, 2.92. MS-ESI (*m*/*z*): 811.8 ([Pt(dtfmbpy)(ttcn)]$(PF_6)^+$), 332.9 ([Pt(dtfmbpy)(ttcn)]$^{2+}$). ^{1}H NMR (CD_3CN, δ): 9.02 (2H, s with Pt satellites, $J_{H-Pt} = 37$ Hz, 6,6′-H), 8.81 (4H, m, 3,3′-H and 4,4′-H), 3.32−3.03 (12H, m, ttcn).

X-ray Crystallography. Orange crystalline blocks of [Pt(bpy)(ttcn)]$(PF_6)_2$ and yellow rectangular blocks of [Pt(4,4′-dmbpy)(ttcn)]$(PF_6)_2$·CH_3CN·H_2O were obtained by evaporation of CH_3CN/H_2O solutions. Orange crystalline blocks of [Pt(5,5′-dmbpy)(ttcn)]$(PF_6)_2$ and red needles of [Pt(dtfmbpy)(ttcn)]$(PF_6)_2$·CH_3CN were obtained from CH_3CN/Et_2O solutions. Single crystals of [Pt(dbbpy)(ttcn)]$(PF_6)_2$·CH_3NO_2 were obtained as yellow irregular plates from a CH_3NO_2/Et_2O solution, whereas single crystals of the same compound containing different solvate molecules, [Pt(dbbpy)(ttcn)]$(PF_6)_2$·$2CH_3CN$·$0.5C_6H_6$, were grown from an acetonitrile/benzene solution.

For X-ray examination and data collection, a suitable crystal of [Pt(bpy)(ttcn)]$(PF_6)_2$ was mounted on the tip of a glass fiber with epoxy resin, whereas crystals of the remaining complexes were each mounted in Cryo-loops with paratone-N and immediately transferred to the goniostat bathed in a cold stream. Intensity data were collected using a Bruker SMART 1K or Bruker SMART6000 CCD diffractometer with graphite-monochromated Mo Kα radiation, $\lambda = 0.71073$ Å, and a detector distance of 5 cm. The data frames were processed using the program SAINT.[18] The data were corrected for decay, Lorentz and polarization effects, and absorption and beam corrections were applied based on the multiscan technique used in SADABS.[19]

The structures were solved by a combination of the Patterson method (direct methods were used for [Pt(bpy)(ttcn)]$(PF_6)_2$) in SHELXTL and the difference Fourier technique. The resulting models were refined by full-matrix least squares on F^2.[20] Non-hydrogen atoms were refined with anisotropic displacement parameters. H atoms of the cations were either located directly or calculated on the basis of geometric criteria and treated with a riding model. The water hydrogens for [Pt(4,4′-dmbpy)(ttcn)]$(PF_6)_2$·CH_3CN·H_2O were located directly and held fixed at that position. The isotropic temperature factors of the H atoms were defined as *a* times U_{eq} of the adjacent atom ($a = 1.5$ for $-CH_3$, $-OH$ and 1.2 for all others). In [Pt(4,4′-dmbpy)(ttcn)]$(PF_6)_2$·CH_3CN·H_2O, one PF_6^- shows typical disorder, and the best disorder model resulted in occupancies in the range 65−74% for the major component. In [Pt(5,5′-dmbpy)(ttcn)]$(PF_6)_2$, one PF_6^- also shows typical disorder, and a reasonable disorder model for F1 and F2 gives occupancies of 75%. In [Pt(dtfmbpy)(ttcn)]$(PF_6)_2$·CH_3CN, the PF_6^- anions show typical disorder, and reasonable disorder models resulted in occupancies in the range 65−70% for the major components. Additionally, one of the $-CF_3$ groups is disordered, and a reasonable disorder model was obtained with the major component having occupancies in the range 65−70%. The anisotropic displacement parameters for the disordered F atoms were held equivalent to the better-behaved F4−F6. The bond distances for the disordered $-CF_3$ group were also restrained to avoid becoming unreasonably short. Crystallographic data are summarized in Table 1.

Results and Discussion

Synthesis. The hexafluorophosphate salts of the five platinum(II) bipyridyl complexes (Chart 1) with the ttcn ligand were synthesized by modification of the procedure of Nikol and co-workers[2] for the preparation of [Pt(phen)(ttcn)]$(PF_6)_2$. The synthesis of [Pt(bpy)(ttcn)]$(PF_6)_2$ is depicted in Scheme 1.

The appropriate Pt(diimine)Cl_2 starting material was refluxed with ttcn for 3 h, during which the solution underwent a dramatic color change from bright yellow to orange or orange/red. After addition of excess NH_4PF_6, slow removal of approximately one-third of the solvent, and cooling to 0 °C, the product precipitated. The yellow, orange, and red PF_6^- salts are air-stable and soluble in polar organic solvents. Their compositions were confirmed by ^{1}H NMR spectroscopy, X-ray crystallography, and elemental analysis. ESI-TOF mass spectra of the salts exhibit peaks consistent

(18) Bruker SMART (v5.054, v5.625, or v5.628) and SAINT (v6.02A, v6.28A, or v6.36A) programs were used for data collection and data processing, respectively. Bruker Analytical X-ray Instruments, Inc., Madison, WI.

(19) SADABS (v2.03, v2.05, or v2.10) was used for the application of semiempirical absorption and beam corrections. Sheldrick, G. M., University of Göettingen, Germany.

(20) SHELXTL (v5.1, v6.1, or v6.12) was used for the structure solution and generation of figures and tables. Sheldrick, G. M., University of Göttingen, Germany, and Bruker Analytical X-ray Instruments, Inc., Madison, WI. Neutral-atom scattering factors were used as stored in this package.

Table 1. Crystallographic Data for [Pt(bpy)(ttcn)]$(PF_6)_2$, [Pt(4,4′-dmbpy)(ttcn)]$(PF_6)_2$·CH_3CN·H_2O, [Pt(5,5′-dmbpy)(ttcn)]$(PF_6)_2$, [Pt(dbbpy)(ttcn)]$(PF_6)_2$·CH_3NO_2, and [Pt(dtfmbpy)(ttcn)]$(PF_6)_2$·CH_3CN

	bpy	4,4′-dmbpy	5,5′-dmbpy	dbbpy	dtfmbpy
formula	$[C_{16}H_{20}N_2S_3Pt](PF_6)_2$	$[C_{18}H_{24}N_2S_3Pt](PF_6)_2$·$CH_3CN$·$H_2O$	$[C_{18}H_{24}N_2S_3Pt](PF_6)_2$	$[C_{24}H_{36}N_2S_3Pt](PF_6)_2$·$CH_3NO_2$	$[C_{18}H_{18}N_2F_6S_3Pt](PF_6)_2$·$CH_3CN$
Fw, g/mol	821.55	908.67	849.60	994.80	998.61
crystal system	triclinic	triclinic	triclinic	triclinic	monoclinic
space group	$P\bar{1}$ (No. 2)	$P\bar{1}$ (No. 2)	$P\bar{1}$ (No. 2)	$P\bar{1}$ (No. 2)	$P2_1/c$ (No. 14)
a, Å	10.2529(3)	10.1895(3)	10.6397(4)	11.5422(7)	13.1187(9)
b, Å	10.7791(3)	11.8566(4)	10.8449(4)	11.6100(7)	20.9031(15)
c, Å	10.7867(3)	13.1004(4)	11.2621(4)	13.6052(9)	11.3815(8)
α, deg	83.886(1)	77.345(1)	90.035(1)	85.902(1)	90
β, deg	87.565(1)	79.967(1)	98.061(1)	89.675(1)	105.789(2)
γ, deg	84.901(1)	72.341(1)	91.283(1)	74.942(1)	90
V, Å^3	1179.99(6)	1461.56(8)	1286.32(8)	1755.90(19)	3003.3(4)
Z	2	2	2	2	4
μ, mm^{-1}	6.453	5.224	5.923	4.359	5.120
ρ_{calc}, g cm^{-3}	2.312	2.065	2.194	1.882	2.209
T, K	150(2)	100(2)	150(2)	150(2)	150(2)
radiation, Å	0.71073	0.71073	0.71073	0.71073	0.71073
no. reflns collcd	16 783	17 480	17 942	18 631	31 161
no. ind reflns/R_{int}	5855/0.0236	5978/0.0260	6392/0.0301	8331/0.0354	6153/0.0634
GOF on F^2	1.09	1.049	1.018	1.058	1.042
R_1/wR_2 [$I > 2\sigma(I)$][a]	0.0174/0.0444	0.0249/0.0638	0.0190/0.0472	0.0306/0.0621	0.0358/0.0767
wR_2 (all data)[a]	0.0181/0.0447	0.0269/0.0650	0.0202/0.0479	0.0383/0.0640	0.0609/0.0882

[a] $R_1 = \sum||F_o| - |F_c||/\sum|F_o|$, w$R_2 = [\sum w(F_o^2 - F_c^2)^2/\sum w(F_o^2)^2]^{1/2}$.

Chart 1. Bipyridyl Ligands

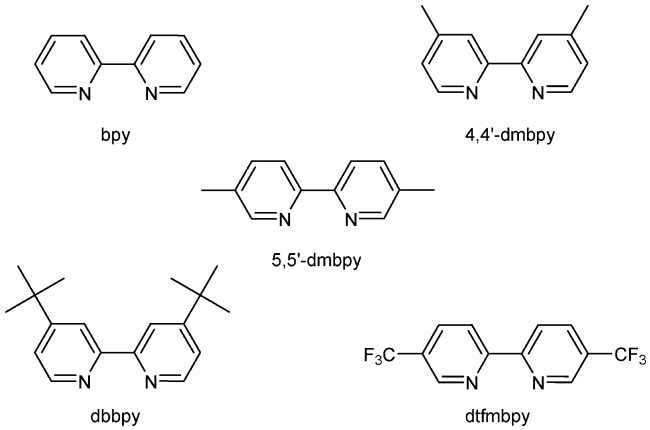

Scheme 1. Synthesis of [Pt(bpy)(ttcn)]$(PF_6)_2$

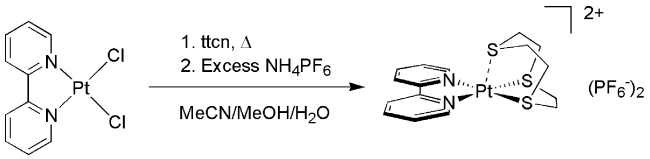

with the loss of one or two PF_6^- anions. In all cases, the observed isotope patterns agreed well with the predicted patterns based on natural isotopic abundancies.

^{1}H NMR Spectroscopy. The proposed C_s symmetry for the dications is consistent with the relatively uncomplicated patterns of resonances in the aromatic and aliphatic regions of the ^{1}H NMR spectra. Assignments for the diimine aromatic resonances were deduced from splitting patterns and the absence of specific resonances from the spectra of the complexes with substituted bipyridyl ligands. The chemical shifts of the aromatic resonances exhibit a characteristic ordering, with the 6,6′-proton resonances shifted furthest downfield (9.02−8.60 ppm), followed by overlapping 3,3′- and 4,4′-proton resonances (8.81−8.21 ppm), and the 5,5′-proton resonances shifted furthest upfield (7.81−7.62 ppm). The distinct ^{195}Pt satellites ($J_{H-Pt} = 35-37$ Hz) of the 6,6′-proton resonances confirm coordination of the bipyridyl ligands to the platinum centers. Overall, the diimine aromatic resonances are shifted furthest downfield for the dtfmbpy complex because of the electron-withdrawing properties of the $-CF_3$ groups. For the 4,4′-dmbpy and 5,5′-dmbpy complexes, resonances attributed to the methyl protons appear at 2.62 and 2.53 ppm, respectively, whereas that of the dbbpy complex occurs at 1.47 ppm. For each complex, the ttcn resonances appear as a multiplet centered near 3.2 ppm, consistent with an AA′BB′ pattern. A similar pattern in the spectrum of $[Pt(phen)ttcn)]^{2+}$ has been attributed to rapid intermolecular exchange involving successive 1,4-metallotropic shifts. Coalescence was reported to occur at approximately −80 °C, indicating a relatively low barrier to exchange (38 kJ/mol).[2] Cooling $[Pt(bpy)(ttcn)]^{2+}$ in deuterated acetone also causes the ttcn signal to broaden and then collapse, establishing that the coalescence occurs at less than −80 °C.

X-ray Crystallography. The structures of the complexes were confirmed by single-crystal X-ray diffraction studies, with crystallographic data summarized in Table 1. Selected bond distances and angles are given in Table 2, and ORTEP diagrams for the cations are shown in Figures 1 and 2.[21]

The cations, hexafluorophosphate anions, and solvent molecules pack as discrete units, and there are no unusually close intermolecular interactions. The structures of the cations in these salts are similar. Each Pt atom is bonded to two N atoms of the bipyridyl ligand and two S atoms of the ttcn in an approximately square planar geometry around the metal center. The ttcn ligand adopts an endodentate geometry and the third sulfur atom forms a weak axial interaction with the Pt atom (2.84−2.97 Å), resulting effectively in a five-

(21) The structures of [Pt(bpy)(ttcn)]$(PF_6)_2$ and [Pt(4,4′-dmbpy)(ttcn)]-$(PF_6)_2$·$2.5CH_3NO_2$ recently have been reported (Grant, G. J.; Patel, K. N.; Helm, M. L.; Mehne, L. F.; Klinger, D. W.; VanDerveer, D. G. *Polyhedron* **2004**, *23*, 1361−1369).

Table 2. Selected Distances (Å) and Angles (deg) for Pt(bipyridyl)(ttcn)$^{2+}$ Complexes

parameter	bpy	4,4′-dmbpy	5,5′-dmbpy	dbbpy	dtfmbpy
Pt−N(1)	2.0530(19)	2.044(3)	2.050(2)	2.040(3)	2.058(5)
Pt−N(2)	2.047(2)	2.060(3)	2.0512(19)	2.043(3)	2.053(5)
Pt−S(1)	2.2627(6)	2.2595(9)	2.2692(6)	2.2755(9)	2.2636(15)
Pt−S(2)	2.2751(5)	2.2725(9)	2.2686(6)	2.2756(9)	2.2758(16)
Pt···S(3)	2.8423(6)	2.957(1)	2.8532(6)	2.965(1)	2.956(2)
N(1)−Pt−N(2)	79.60(8)	79.40(12)	79.70(8)	79.02(11)	79.6(2)
N(1)−Pt−S(1)	94.80(6)	93.96(9)	96.04(6)	95.68(8)	94.38(15)
N(1)−Pt−S(2)	170.05(6)	171.23(8)	173.13(6)	171.20(8)	171.19(15)
N(2)−Pt−S(1)	173.41(6)	173.00(9)	169.80(6)	172.25(8)	171.44(15)
N(2)−Pt−S(2)	96.66(6)	97.81(9)	94.99(6)	96.37(8)	96.82(16)
S(1)−Pt−S(2)	88.30(2)	88.43(3)	88.47(2)	88.12(3)	88.23(6)
N(1)−Pt−S(3)	103.58(6)	104.46(8)	100.50(6)	105.06(8)	105.9(2)
N(2)−Pt−S(3)	99.09(6)	100.36(8)	103.88(6)	104.06(8)	103.7(2)
S(1)−Pt−S(3)	85.56(2)	83.35(3)	85.96(2)	82.70(3)	83.73(6)
S(2)−Pt−S(3)	86.07(2)	84.18(3)	84.95(2)	83.27(3)	82.72(6)

coordinate metal center (Figure 2). The N1−Pt−N2 angles are less than 90° (79.0−79.7°), in accord with the bite angles of the chelating bipyridyl ligands. The S1−Pt−S2 angles (88.1−88.5°) are closer to 90°, in agreement with related complexes.[2] The resulting N−Pt−S angles are obtuse, ranging from 94.0° to 97.8°. The Pt−N1 and Pt−N2 distances are very similar for the five compounds, ranging from 2.04 to 2.06 Å, as are the equatorial Pt−S1 and Pt−S2 bond distances, which vary from 2.26 to 2.28 Å. Overall, the Pt−N distances are similar to those of platinum(II) bipyridyl dithiolate complexes (2.02−2.07 Å).[22−26] However, as expected, the Pt−S bond distances are significantly longer than those observed for the diimine dithiolate complexes (2.24−2.26 Å).

To gain further insight into the structures of the cations, we have used the approach of Muetterties and Guggenberger[27] for describing five-coordinate complexes in terms of the nine dihedral angles between the normals to the planes sharing a common edge in idealized polyhedra. Holmes and Deiters[28] have suggested that deviations of these angles from idealized values for trigonal bipyramid (TBP) and square pyramid (SQP) geometries can provide a measure of the displacement along the Berry pseudorotation coordinate describing the interconversion between these geometries.[29] This analysis shows that the five [Pt(bipyridyl)(ttcn)]$^{2+}$ complexes are distorted by 77−80% away from a TBP structure, firmly establishing these compounds as having approximate SQP geometries (Figure S1). We have found that 16 of 17 published structures of platinum(II) complexes with endodentate ttcn ligands[2,4−12] are similarly distorted (83(6)°). The lone outlier is the cation in crystals of [Pt(PPh$_3$)$_2$(ttcn)](PF$_6$)$_2$·2CH$_3$NO$_2$,[4] which adopts a structure intermediate between idealized TBP and SQP geometries (Figure S1). It should be noted that the majority of the 22 complexes do not lie exactly on the Berry coordinate, presumably because of steric and electronic demands of the ligands. We also have found that, for the bipyridyl complexes reported here, the average trans-basal angle is 173(1)°, in good agreement with that observed for the other Pt(II) ttcn structures (173(4)°). The average difference (*d*) between the Pt···S3 distance and the equatorial Pt−S distances is 0.64(6) Å for the five bipyridyl complexes. Thus, using the criteria of Auf der Heyde and Bürgi[30] developed for five-coordinate d^8 metal complexes, we can firmly classify these complexes as having flattened SQP structures, characterized by large trans-basal angles and relatively long apical metal−ligand interactions.

A more detailed analysis of these Pt(II) ttcn structures provides compelling support for the proposal by Nikol and co-workers[2] that there exists a correlation between the apical Pt···S3 interaction and the donor properties of the ancillary ligands. The Pt···S3 distances (2.84−2.97 Å) for the bipyridyl complexes are similar to that reported for [Pt(phen)(ttcn)]$^{2+}$ (2.821(3) Å)[2] and are clustered tightly within the comparatively wide range of values (2.64−3.26 Å) reported for other Pt(II) complexes with ttcn ligands.[4−13] In our analysis, we have found that a shortening of the Pt···S3 distance is generally accompanied by an increase in the displacement of the Pt atom (*x*) from the coordination plane defined by the four ligands. This correlation is graphically illustrated in Figure 3, which shows the dependence of the displacement on the difference (*d*) between the Pt···S3 distance and the average of the two equatorial Pt−S distances for each Pt(II) ttcn complex. From these data, it is apparent that complexes with ancillary phosphine ligands tend to have the shortest apical Pt···S3 distances (2.64−2.87 Å), whereas those with halide ligands tend to have the longest apical contacts (3.21−3.26 Å). The mixed ligand system, [Pt(ttcn)(PPh$_3$)Cl]$^+$, lies between these regions (3.08 Å). Grant and co-workers[8] have noted that this trend is in keeping with the relative π-acceptor properties of the ancillary ligands.

(22) Adams, C. J. *J. Chem. Soc., Dalton Trans.* **2002**, 1545−1550.
(23) Connick, W. B.; Gray, H. B. *J. Am. Chem. Soc.* **1997**, *119*, 11620−11627.
(24) Keefer, C. E.; Bereman, R. D.; Purrington, S. T.; Knight, B. W.; Boyle, P. D. *Inorg. Chem.* **1999**, *38*, 2294−2302.
(25) Kubo, K.; Nakano, M.; Tamura, H.; Matsubayashi, G. *Inorg. Chim. Acta* **2002**, *336*, 120−124.
(26) Smucker, B. W.; Hudson, J. M.; Omary, M. A.; Dunbar, K. R. *Inorg. Chem.* **2003**, *42*, 4714−4723.
(27) Muetterties, E. L.; Guggenberger, L. J. *J. Am. Chem. Soc.* **1974**, *96*, 1748−1756.
(28) Holmes, R. R.; Deiters, J. A. *J. Am. Chem. Soc.* **1977**, *99*, 3318−3326.
(29) We have adopted the convention of Auf der Heyde and Nassimbeni by choosing the idealized SQP to have axial-basal angles of 105°.
(30) Auf der Heyde, T. P. E.; Bürgi, H. B. *Inorg. Chem.* **1989**, *28*, 3982−3989.

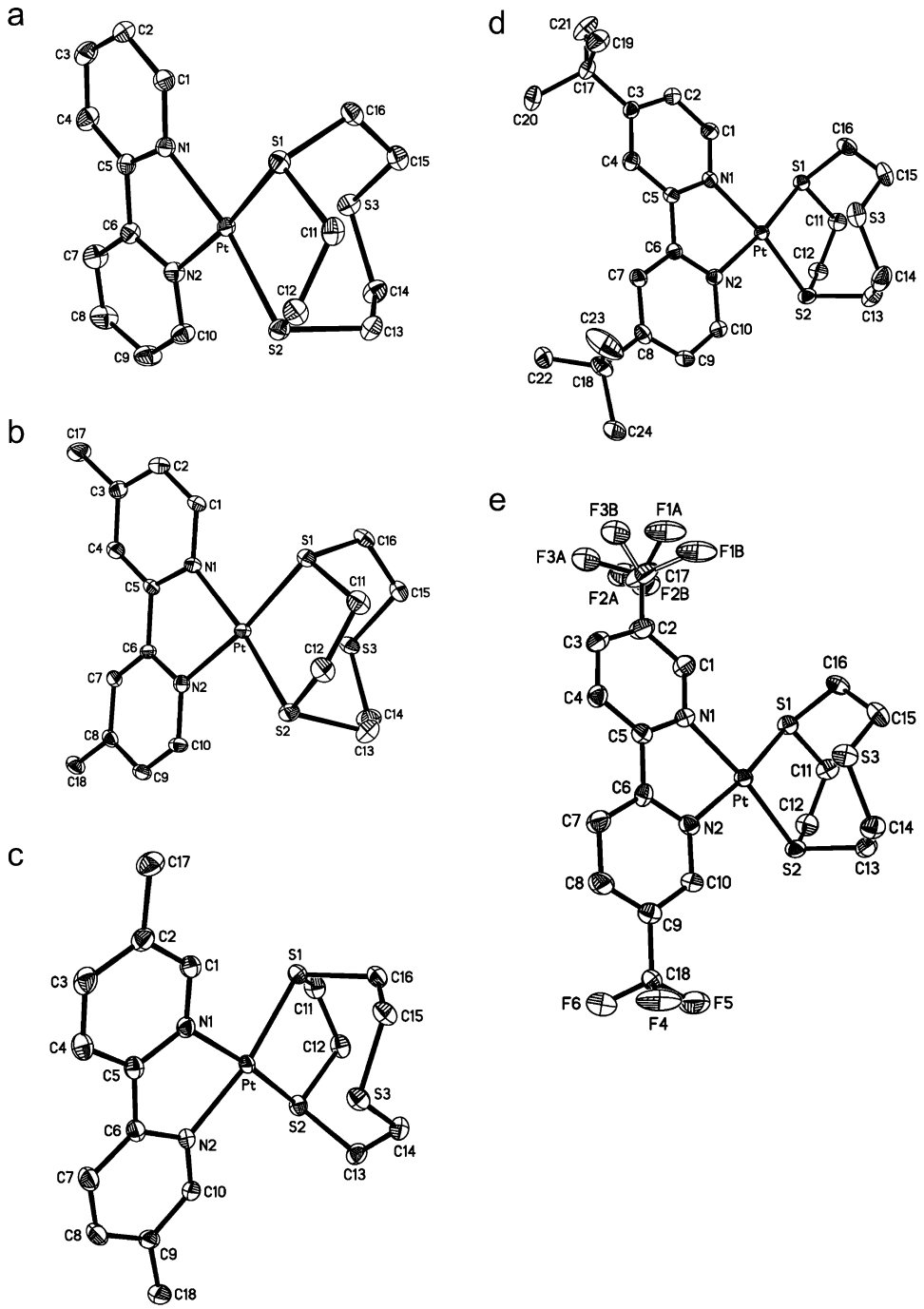

Figure 1. ORTEP drawings of cations in (a) [Pt(bpy)(ttcn)]$(PF_6)_2$, (b) [Pt(4,4′-dmbpy)(ttcn)]$(PF_6)_2 \cdot CH_3CN \cdot H_2O$, (c) [Pt(5,5′-dmbpy)(ttcn)]$(PF_6)_2$, (d) [Pt(dbbpy)(ttcn)]$(PF_6)_2 \cdot CH_3NO_2$, and (e) [Pt(dtfmbpy)(ttcn)]$(PF_6)_2 \cdot CH_3CN$.

Increased π-acceptor character of phosphine groups, as compared to π-donor halide ligands, increases the positive charge on the platinum center and favors increased electrostatic and charge-transfer interactions between the metal and the apical sulfur. Interestingly, for the bis-halide complexes, *d* decreases along the series $I^- > Br^- > Cl^-$, as expected based on electronegativities, but in contradiction to the relative donor strengths of these ligands.[31] To account for the complexes with strong π-acceptor diimine ligands having apical distances intermediate to those of the phosphine and halide derivatives, it is necessary to amend this model to incorporate the σ-donor effect of the ancillary ligands. Although the phen and the bipyridyl ligands are strong π-acceptors, they also are strong σ-donors. Thus, the longer Pt···S3 distances for complexes with these ligands, as compared to those with phosphine groups, is consistent with the expected increased electron density on the metal center. Indeed, the importance of the σ-donor capacity of the ancillary ligands is illustrated by the structure of Pt(ttcn)$(Ph)_2$. In that case, the ttcn adopts an exodentate geometry with S3 directed away from the metal (Pt···S3, 4.103(2) Å),[10] reflecting comparatively high electron density on the platinum center.

(31) Caulton, K. G. *New J. Chem.* **1994**, *18*, 25−41.

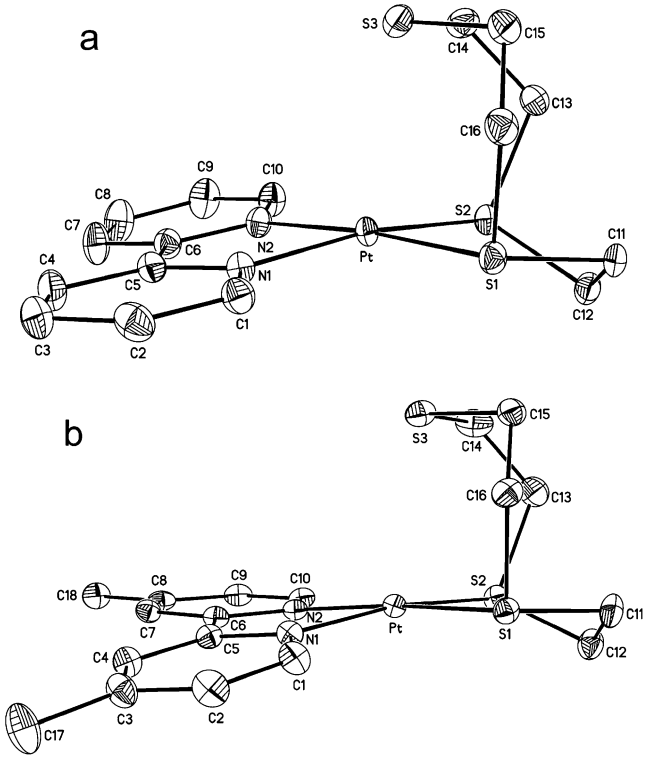

Figure 2. ORTEP drawings of cations in (a) $[Pt(bpy)(ttcn)](PF_6)_2$ and (b) $[Pt(4,4'\text{-dmbpy})(ttcn)](PF_6)_2 \cdot CH_3CN \cdot H_2O$, showing the endodentate configuration of the ttcn ligand.

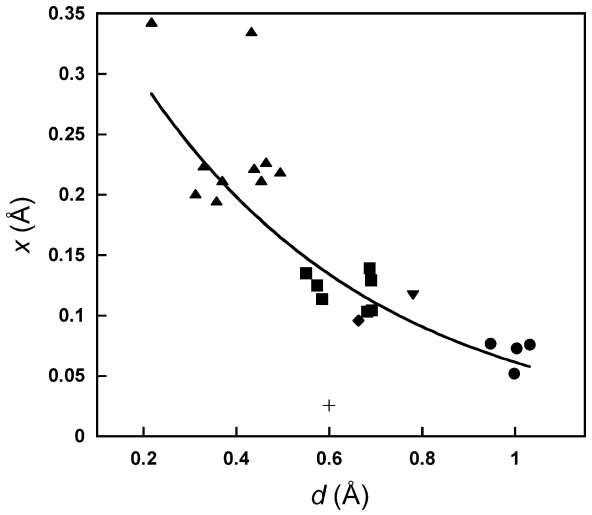

Figure 3. Dependence of the displacement (x) of the Pt atom from the coordination plane on the difference (d) between the Pt···S3 distance and the average of the two equatorial Pt−S bond lengths for 22 Pt(II) ttcn complexes with phosphine (▲),[4−6,9] diimine (■) (this work and ref 2), and halide (●)[8,11] ligands. Data for $[Pt(ttcn)_2](PF_6)_2$ (+),[12] Pt(ttcn)(Ph)Cl (▼),[7] and Pt(2,5,8-trithia[9](2,9)-1,10-phenanthroline)$](PF_6)_2$ (◆)[13] also are included. The curve represents the best-fit exponential for the 22 ttcn complexes: $x = 0.43e^{-1.95d}$.

For the diimine complexes, the Pt···S3 distance increases along the series phen < bpy ≈ 5,5′-dmbpy < dtfmbpy ≈ 4,4′-bpy ≈ dbbpy. From the preceding analysis, it is intriguing to consider the possibility that this variation reflects the relative donor properties of the diimine ligands, in addition to crystal packing forces.[32] In the case of $[Pt(phen)(ttcn)]^{2+}$, which has the shortest apical contact, it is noteworthy that phen is a better π-acceptor than bpy and therefore would be expected to favor the observed shorter Pt···S3 contact. Comparatively longer contacts for complexes with alkyl substituents at the 4 and 4′ positions of the bipyridyl ligand (4,4′-dmbpy and dbbpy) also are in keeping with the expected increased σ-donor properties of these ligands as compared to bpy. On the other hand, the Pt···S3 distance for the 5,5′-dmbpy complex is only ∼0.01 Å longer than that of the bpy complex, as might be expected for relatively weak directing properties of alkyl substituents at the 5 and 5′ positions (i.e., meta with respect to the N donor atom). Interestingly, the dtfmbpy complex would be expected to be the weakest σ-donor and strongest π-acceptor in this series of diimine ligands, yet this complex exhibits a comparatively long Pt···S3 distance (2.956(2) Å).

From application of the structure correlation principle,[33] we regard the correlation in Figure 3 as a map of the reaction coordinate for an association reaction at a planar four-coordinate Pt center to give a five-coordinate SQP species. From an exponential fit, we can derive an expression in Pauling's formalism relating changes in bond length to bond number:[34]

$$d = -1.18 \log(x/0.43) \qquad (1)$$

where $x/0.43$ provides a measure for the bond number. These results are remarkably similar to those obtained by Auf der Heyde and Nassimbeni[35] for five-coordinate nickel complexes, which have an apparent bond number given by $x/0.44$. However, in the present case, the correlation between d and the donor properties of the ancillary ligands leads us to suggest that Figure 3 also serves to map the early stages of the reaction coordinate for oxidation of a four-coordinate Pt(II) center to give a five-coordinate SQP Pt(III) product. Decreasing electron density at the metal center causes increased pyramidalization and stronger interaction with an incoming nucleophile. Interestingly, of the complexes examined here, only $[Pt(ttcn)_2]^{2+}$ is known to undergo facile outer-sphere oxidation at low potentials (0.32 V vs Fc/Fc^+).[36] This complex also is a significant outlier in Figure 3 and may, in effect, lie on a different reaction coordinate if the six-coordinate Pt(III) adduct lies at lower energy than the five-coordinate SQP Pt(III) product.

Electronic Structures. To better understand the electronic structures of these compounds, we have examined their absorption, emission, and electrochemical properties. The compounds readily dissolve to give yellow solutions that strongly absorb in the UV region (Table 3 and Figure 4). At first glance, the absorption spectra in acetonitrile solution

(32) Evidence in support of this notion is tenuous. Both crystals of Pt(dbbpy)$(ttcn)^{2+}$ gave similar shortest apical Pt···S distances (2.965(1) and 2.956(2) Å); however, greater variation was found for different crystals containing $Pt(ttcn)Cl_2$ (3.226(3) and 3.260(3) Å) (refs 8 and 11) and for crystals containing $[Pt(ttcn)_2](PF_6)_2$ (2.88−3.07 Å) (ref 12 and Green, T. W.; Krause Bauer, J. A.; Connick, W. B., manuscript in preparation).

(33) Bürgi, H.-B., Dunitz, J. D., Eds. *Structure Correlation*; Verlagsgesellschaft: Weinheim, 1994; Vol. 1.
(34) Pauling, L. *J. Am. Chem. Soc.* **1947**, *69*, 542−553.
(35) Auf der Heyde, T. P. E.; Nassimbeni, L. R. *Inorg. Chem.* **1984**, *23*, 4525−4532.
(36) Schröder, M. *Pure Appl. Chem.* **1988**, *60*, 517−524.

Table 3. UV−Visible Spectroscopic Data (λ, nm) and Band Assignments for Pt(diimine)(ttcn)$^{2+}$ Complexes in Acetonitrile [ϵ, M^{-1} cm^{-1}], 77 K 3:1 EtOH/MeOH Glassy Solution Excitation and Emission Maxima (nm), and Cathodic Peak Reduction Potentials (V vs Ag/AgCl)

compound	$^1(\pi\rightarrow\pi_1^*)$	^{1}MLCT	emission maxima	excitation maxima	cathodic reduction
[Pt(bpy)(ttcn)](PF$_6$)$_2$	317 [12 300]	398 [2200]	620	420sh, 454, 475sh	−0.87
[Pt(4,4′-dmbpy)(ttcn)](PF$_6$)$_2$	309, 318 [12 900, 13 200]	385 [2400]	615	455	−0.85
[Pt(5,5′-dmbpy)(ttcn)](PF$_6$)$_2$	326, 338 [14 200, 12 600]	387 [2300]	605	453, 470	−0.92
[Pt(dbbpy)(ttcn)](PF$_6$)$_2$	310, 319 [12 800, 12 900]	387 [2500]	570, 600sh	448	−0.95
[Pt(dtfmbpy)(ttcn)](PF$_6$)$_2$	309 [9800]	460 [1300]	645	450sh, 480, 517	−0.46

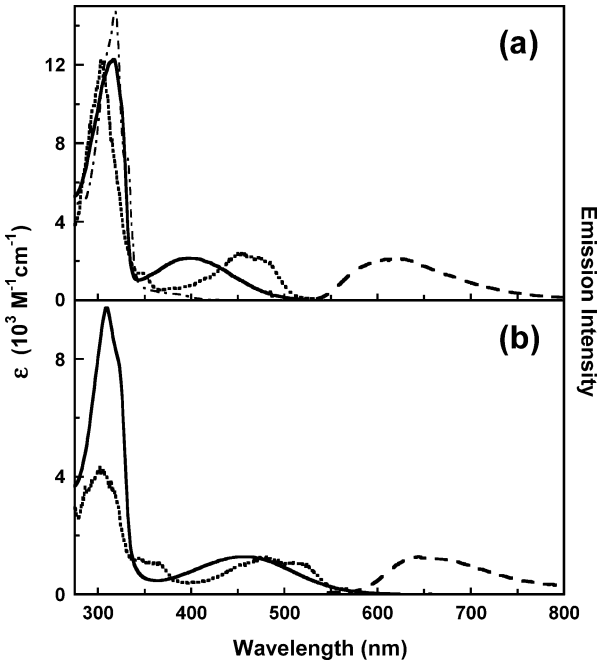

Figure 4. (a) UV−visible absorption spectrum (−) of Pt(bpy)(ttcn)$^{2+}$ in acetonitrile solution with normalized 77 K 3:1 EtOH/MeOH glassy solution excitation (·····) and emission (− − −) spectra. The absorption spectrum of Pt(bpy)(1,4-dithn)$^{2+}$ also is shown (− - − -). (b) UV−visible absorption spectrum (−) of Pt(dtfmbpy)(ttcn)$^{2+}$ in acetonitrile solution with normalized 77 K 3:1 EtOH/MeOH glassy solution excitation (·····) and emission (− − −) spectra.

appear very similar to those of other platinum(II) bipyridyl complexes.[14] An intense, structured, and solvent-insensitive absorption band maximizing near 310−340 nm (10 000−14 000 M^{-1} cm^{-1}) is attributed to the lowest diimine-centered spin-allowed $\pi-\pi_1^*$ transition. Interestingly, the bands in the spectra of the bpy and 4,4′-substituted bipyridyl derivatives occur at very similar wavelengths with the first vibronic feature at ∼320 nm. In contrast, this transition is more intense and shifted by ∼1700 cm^{-1} to the red in the spectrum of the 5,5′-dmbpy analogue (Table 3). We have found stabilization of the lowest singlet $\pi-\pi^*$ state of 5,5′-dmbpy complexes to be a general result,[37] and our observations are consistent with the influence of hyperconjugation on $\pi-\pi^*$ transitions as described by Mulliken for cyclic dienes.[38] Mixing of orbitals centered on the methyl carbon with the bipyridyl π levels will tend to red-shift and increase the oscillator strength of the lowest $\pi-\pi^*$ transition.[39] The effect is more pronounced for 5,5′-substituents because these lie along the axis of polarization and are favorably situated for resonance interaction.[40] Similar trends are observed for substituted biphenyl compounds. For example, the $\pi-\pi^*$ band maxima for 3,3′- and 4,4′-dimethyl biphenyl derivatives are shifted by ∼400 and ∼1300 cm^{-1}, respectively, from that of biphenyl.[41−43] As expected for bipyridyl complexes,[44−46] the intense $\pi-\pi_2^*$ transition, involving the next lowest bipyridyl-centered π^* level, appears as a shoulder near 250 nm (12 500−21 000 M^{-1} cm^{-1}). The band maximum is well-resolved, more intense, and slightly red-shifted in the spectrum of the 5,5′-dmbpy complex (255 nm, 22 900 M^{-1} cm^{-1}).

A very broad and solvent-sensitive absorption band with full-width-at-half-maximum (fwhm) of ∼6400 cm^{-1} is centered at 460 nm (1300 M^{-1} cm^{-1}) in the spectrum of the dtfmbpy derivative. The maximum is shifted to considerably shorter wavelengths in the spectra of the bpy (398 nm, 2200 M^{-1} cm^{-1}; fwhm, ∼6600 cm^{-1}) and dialkyl-substituted bipyridyl (385−387 nm, 2300−2400 M^{-1} cm^{-1}) complexes, suggesting a charge-transfer transition involving the diimine.[47] In point of fact, these energies, intensities, and substituent effects are consistent with a predominantly spin-allowed metal-to-ligand(bipyridyl) charge-transfer (MLCT) transition, and a similar band has been observed for other platinum(II) bipyridyl complexes.[14,45,46,48−50] Electron-withdrawing substituents on the bipyridyl ligand are expected to stabilize MLCT states, whereas donating substituents are expected to destabilize these states, in keeping with the observed energy trend: dtfmbpy < bpy < dbbpy ≈ 5,5′-dmbpy ≈ 4,4′-dmbpy. In an effort to confirm these effects, we have recorded the cyclic voltammograms of each complex in 0.1 M $TBAPF_6$ acetonitrile solution. None of the complexes is oxidized at potentials <2.0 V vs Ag/AgCl (3.0 M NaCl), in accord with the high oxidation potentials of other platinum(II) diimine complexes.[48,51−54] In contrast,

(37) Green, T. W.; Connick, W. B., unpublished results.
(38) Mulliken, R. S. *J. Chem. Phys.* **1939**, *7*, 339−352.
(39) Jaffé, H. H.; Orchin, M. *Theory and Applications of Ultraviolet Spectroscopy*; John Wiley and Sons: New York, 1962.
(40) Taking the Pt(II) bipyridyl complex to lie in the *xz* plane in local C_{2v} symmetry, the $\pi-\pi^*$ band is associated with the $A_1\rightarrow B_1$ transition, which is polarized along the long axis of the ligand.
(41) O'Shaughnessy, M. T.; Rodebush, W. H. *J. Am. Chem. Soc.* **1940**, *62*, 2906−2911.
(42) Suzuki, H. *Bull. Chem. Soc. Jpn.* **1959**, *32*, 1350−1356.
(43) Beaven, G. H.; Johnson, E. A. *Spectrochim. Acta* **1959**, *14*, 67−81.
(44) Kober, E. M.; Meyer, T. J. *Inorg. Chem.* **1982**, *21*, 3967−3977.
(45) Gidney, P. M.; Gillard, R. D.; Heaton, B. T. *J. Chem. Soc., Dalton Trans.* **1973**, 132−134.
(46) Connick, W. B.; Miskowski, V. M.; Houlding, V. H.; Gray, H. B. *Inorg. Chem.* **2000**, *39*, 2585−2592.
(47) The possibility of charge-transfer involving the metal and ttcn ligand is unlikely because Pt(ttcn)$_2^{2+}$ only absorbs weakly in this region.
(48) Collison, D.; Mabbs, F. E.; McInnes, E. J. L.; Taylor, K. J.; Welch, A. J.; Yellowlees, L. *J. Chem. Soc., Dalton Trans.* **1996**, 329−334.
(49) Miskowski, V. M.; Houlding, V. H. *Inorg. Chem.* **1989**, *28*, 1529−1533.
(50) Miskowski, V. M.; Houlding, V. H.; Che, C.-M.; Wang, Y. *Inorg. Chem.* **1993**, *32*, 2518−2524.

platinum(II) diimine dithiolate complexes are oxidized at more modest potentials (<1 V),[23,55] confirming significant involvement of the electron-rich thiolate groups in those processes. Each of our ttcn complexes exhibits an irreversible reduction at >−1 V, whereas other platinum(II) bipyridyl complexes undergo reversible diimine-centered reductions near these potentials.[48,51−60] Although strict thermodynamic data are not available, it is noteworthy that the cathodic peak potential for the dtfmbpy complex is shifted by +0.41 V (3300 cm^{-1}) from that of the bpy complex, in excellent agreement with the difference between the reversible reduction potentials for $Ru(bpy)_2(dtfmbpy)^{2+}$ and $Ru(bpy)_3^{2+}$ (0.42 V).[61]

The energies of the MLCT band maxima point to the influence of apical Pt···S3 interactions on the electronic structures of these complexes. It is well known that the lowest MLCT absorption maximum of four-coordinate platinum(II) diimine complexes is very sensitive to the donor properties of the ancillary ligands.[14,46] For strong field, neutral amine groups, the band maximum is shifted to <330 nm (>30 000 cm^{-1}) and buried under the $\pi-\pi_1^*$ band (e.g., Pt(bpy)(en)$^{2+}$),[49] whereas strong σ-donor phenyl groups result in maxima >415 nm (<24 000 cm^{-1}) (e.g., $Pt(bpy)(Ph)_2$; CH_3CN: 434 nm, 2400 M^{-1} cm^{-1}).[56] Therefore, it is not surprising that the MLCT maxima for these ttcn complexes are blue-shifted from the lowest charge-transfer bands of platinum(II) diimine dithiolate complexes.[23,55] For example, the maximum for Pt(4,4′-dmbpy)(ttcn)$^{2+}$ (385 nm) is shifted by 4300 cm^{-1} from that observed for the lowest charge-transfer band of Pt(4,4′-dmbpy)(1,2-ethanedithiolate) (CH_3CN: 462 nm),[62] as expected for the relative electron-donor capacities of the sulfur chelates and significant ligand-to-ligand charge-transfer character for the dithiolate complex. However, it is at first glance surprising that the maximum for Pt(bpy)(ttcn)$^{2+}$ (CH_3OH, 404 nm; DMF, 409 nm) is slightly red-shifted from that observed for complexes with negatively charged ancillary ligands such as moderate σ-donor pyrazolyl groups (e.g., $Pt(bpy)(dmpz)_2$, CH_3OH: 379 nm)[46] and π-donor halide ligands (e.g., $Pt(bpy)Cl_2$, CH_3OH, 370 nm; DMF, 390 nm; $Pt(bpy)Br_2$; DMF, 395 nm).[50] The corresponding MLCT transition in the spectrum of the model complex Pt(bpy)(1,4-dithn)$^{2+}$ must occur at considerably shorter wavelengths because that compound only absorbs weakly at λ > 350 nm (<700 M^{-1} cm^{-1}; Figure 4). Thus, our data establish that binding of neutral ttcn to the Pt(bpy)$^{2+}$ fragment results in a remarkable stabilization of the MLCT state, most likely as a consequence of interactions of the apical sulfur group with the acidic metal center. These interactions are expected to stabilize the MLCT transition state by sulfur lone-pair to vacant 6s/6p(Pt) charge-transfer interactions, as well as sulfur lone-pair/5d(Pt) electron−electron repulsions. Interestingly, in contrast to the pyrazolate and halide derivatives, the absorption band is unstructured in all investigated solvents, as might be expected for a distribution of Pt···S apical contacts associated with rapidly interconverting conformers. In addition, the solvent dependence of the MLCT band maximum is more erratic and weaker than observed for $Pt(bpy)Cl_2$ and the lowest charge-transfer band of platinum(II) diimine dithiolate complexes. For example, over a selection of non-hydroxylic solvents, the energy of the band maximum of $Pt(bpy)Cl_2$ shows a strong linear correlation with Reichardt's $E_T(30)$ parameter[45,63,64] with a slope of 237 $kcal^{-1}$ cm^{-1} mol and correlation coefficient (R^2) of 0.98. For Pt(bpy)(ttcn)$^{2+}$, the slope is 82 $kcal^{-1}$ cm^{-1} mol with $R^2 = 0.11$.[65] Taken together, these data suggest that the Pt···S interactions can be perturbed by solvation effects.

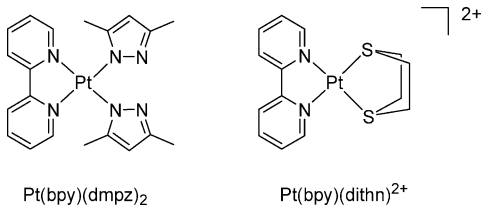

$Pt(bpy)(dmpz)_2$ $Pt(bpy)(dithn)^{2+}$

The preceding considerations lead to the suggestion that, after crudely accounting for differences in the bipyridyl ligand π^* energies and donor properties, the absorption band maxima provide an indication of the relative strengths of the Pt···S apical interactions. This analysis leads to the conclusion that these interactions are enhanced in solutions of Pt(dtfmbpy)(ttcn)$^{2+}$ as compared to the other complexes. To illustrate this point, we can obtain estimates of the relative electronic properties of the bpy and dtfmbpy ligands from accumulated electrochemical and spectroscopic data for related six-coordinate ruthenium complexes, $Ru(bpy)_3^{2+}$ and $Ru(bpy)_2(dtfmbpy)^{2+}$.[61,66] As was alluded to earlier, cyclic voltammetry measurements (0.1 M TBA(ClO_4) acetonitrile) confirm a 3400 cm^{-1} (0.42 eV) stabilization of the π^*(dtfmbpy) relative to π^*(bpy). However, the oxidation potential of $Ru(bpy)_2(dtfmbpy)^{2+}$ also exhibits a 0.17 V (1400 cm^{-1}) cathodic shift from that of $Ru(bpy)_3^{2+}$, reflecting

(51) Braterman, P. S.; Song, J.-I.; Wimmer, F. M.; Wimmer, S.; Kaim, W.; Klein, A.; Peacock, R. D. *Inorg. Chem.* **1992**, *31*, 5084−5088.
(52) Klein, A.; Kaim, W. *Organometallics* **1995**, *14*, 1176−1186.
(53) Hissler, M.; Connick, W. B.; Geiger, D. K.; McGarrah, J. E.; Lipa, D.; Lachicotte, R. J.; Eisenberg, R. *Inorg. Chem.* **2000**, *39*, 447−457.
(54) Kvam, P.-I.; Puzyk, M. V.; Balashev, K. P.; Songstad, J. *Acta Chem. Scand.* **1995**, *49*, 335−343.
(55) Cummings, S. D.; Eisenberg, R. *J. Am. Chem. Soc.* **1996**, *118*, 1949−1960.
(56) Klein, A.; Hausen, H. D.; Kaim, W. *J. Organomet. Chem.* **1992**, *440*, 207−217.
(57) Braterman, P. S.; Song, J. I.; Vogler, C.; Kaim, W. *Inorg. Chem.* **1992**, *31*, 222−224.
(58) Kotlyar, V. S.; Balashov, K. P. *Russ. J. Electrochem. (Translation from Elektrokhimiya)* **1996**, *32*, 1253−1257.
(59) Wan, K.-T.; Che, C.-M.; Cho, K.-C. *J. Chem. Soc., Dalton Trans.* **1991**, 1077−1080.
(60) Che, C.-M.; Wan, K.-T.; He, L.-Y.; Poon, C.-K.; Yam, V. W.-W. *J. Chem. Soc., Chem. Commun.* **1989**, 943−944.
(61) Furue, M.; Maruyama, K.; Oguni, T.; Naiki, M.; Kamachi, M. *Inorg. Chem.* **1992**, *31*, 3792−3795.
(62) Zuleta, J. A.; Bevilacqua, J. M.; Proserpio, D. M.; Harvey, P. D.; Eisenberg, R. *Inorg. Chem.* **1992**, *31*, 2396−2404.
(63) Reichardt, C. *Chem. Rev.* **1994**, *94*, 2319−2358.
(64) For the lowest charge-transfer band of Pt(bpy)(1,2-benzenedithiolate), linear correlation with $E_T(30)$ yields a slope of 205 $kcal^{-1}$ cm^{-1} mol with $R^2 = 0.98$.
(65) Pt(bpy)(ttcn)$^{2+}$: acetone (401 nm), DMF (409 nm), DMSO (412 nm), acetonitrile (409 nm), and nitromethane (395 nm).
(66) Maestri, M.; Grätzel, M. *Ber. Bunsen-Ges. Phys. Chem.* **1977**, *81*, 504−507.

the stabilization of the metal levels due to the weaker donor properties of the dtfmbpy ligand. Consequently, the lowest 4d(Ru)-π^*(dtfmbpy) absorption for $Ru(bpy)_2(dtfmbpy)^{2+}$ (480sh nm) in methanol is shifted by only $\sim$1200 cm^{-1} to the red of that observed for $Ru(bpy)_3^{2+}$ (453 nm). In sharp contrast, the MLCT absorption maximum for Pt(dtfmbpy)-$(ttcn)^{2+}$ is shifted by 3400 cm^{-1} from that of the bpy derivative, in good agreement with the relative cathodic peak potentials. This result points to the synergistic influence of the dtfmbpy ligand on the energy of the MLCT state of Pt-$(dtfmbpy)(ttcn)^{2+}$. Although the relative stabilization of the π^*(dtfmbpy) level is partly responsible for the low energy of the MLCT state, an additional contribution results from apical Pt···S interactions, which are likely enhanced by the more weakly donating dtfmbpy ligand and increased acidity of the Pt center. These interactions evidently largely offset the influence of the weaker donor properties of dtfmbpy on the MLCT energy. However, it is noteworthy that the apical Pt···S3 contacts for the dtfmbpy complex are not especially short in the solid state, suggesting that these interactions may be perturbed by competing packing forces. For example, we find that crystalline samples of the bpy and 5,5′-dmbpy complexes are distinctly orange, whereas the 4,4′-dmbpy and dbbpy derivatives are yellow and yellow-orange, respectively. There are no short intermolecular contacts in any of these crystals, and these color variations cannot reasonably be attributed to diimine···diimine or Pt···Pt interactions. The observations are qualitatively consistent with relative stabilization of the MLCT transition of the bpy and 5,5′-dmbpy samples, in accord with a $\sim$0.1 Å shorter Pt···S3 interaction. The Pt···S3 contact in crystals of the dtfmbpy complex also is significantly longer than observed for the bpy and 5,5′-dmbpy derivatives. Nevertheless, this solid also is distinctly red, and stabilization of the MLCT transition is largely attributable to the low energy of the π^*(dtfmbpy) level, rather than enhanced Pt···S interactions.

Emission measurements also indicate that apical Pt···S interactions significantly influence the electronic structures of these complexes. Although none of the ttcn adducts is luminescent in fluid solution, each exhibits weak emission in 77 K glassy 3:1 EtOH:MeOH solution (Table 3; Figure 4). The emission maxima (570−620 nm) and emission onsets (525−540 nm) of the bpy and dialkyl-substituted bipyridyl complexes are shifted by 600−2000 cm^{-1} to the blue of those observed for the dtfmbpy complex. The emission bands are characteristically broad and asymmetric with profiles suggestive of poorly resolved vibronic structure. Thus, the emission onsets are shifted to the red of those observed for $\pi-\pi^*$ emissions from platinum(II) bipyridyl complexes ($\sim$450 nm), and the bandshapes lack the well-resolved structure associated with those ligand-centered transitions.[46] Likewise, these emissions do not have the characteristic symmetric profile and large Stokes shift typically observed for ligand field emissions (e.g., $Pt(bpy)Cl_2$; solid-state: 641 nm).[49] We conclude that the emissions most likely originate from a lowest, predominantly spin-forbidden MLCT state involving the diimine ligand, as noted for several other platinum(II) bipyridyl systems.[46,50,52,53,56,67−70] In keeping with this assignment, the dtfmbpy derivative exhibits the lowest energy emission in this series, as expected for stabilization of the diimine π^* level by electron-withdrawing trifluoromethyl substituents. Similarly, the emissions from the dialkyl-substituted derivatives occur at slightly higher energies than observed for the bpy complex.

Interestingly, these long-wavelength emission maxima lie well within the range of those observed for platinum(II) diimine dithiolate complexes.[55] For example, the maximum for $Pt(4,4'\text{-dmbpy})(ttcn)^{2+}$ (615 nm) is within 300 cm^{-1} of that observed for Pt(4,4′-dmbpy)(1,2-ethanedithiolate) (624 nm, 1:1:1 DMF:CH_2Cl_2:MeOH, 77 K).[62] This result contrasts sharply with the room-temperature absorption spectra for these two compounds, which show a 4300 cm^{-1} gap between lowest charge-transfer band maxima. Taken together, these observations are consistent with enhancement of apical Pt···S interactions in frozen solution, as compared to fluid solution.

The excitation spectrum of each complex exhibits a well-resolved, low-energy band, maximizing between 450 and 480 nm. For the bpy, 5,5′-dmbpy, and dtfmbpy complexes, the band profiles display characteristic vibronic structure, in keeping with the assignment as a MLCT transition. Although the emissive MLCT state does not necessarily have the same orbital parentage as this spin-allowed excitation band, it is reassuring that the excitation maxima roughly parallel the energy trend observed for the emission maxima: dtfmbpy < 4,4′-dmbpy $\approx$ bpy < 5,5′-dmbpy < dbbpy. In contrast to the room-temperature solution absorption data, the 1200 cm^{-1} gap between the excitation maxima for the bpy and dtfmbpy complexes is in good agreement with the $\sim$1200 cm^{-1} difference between the absorption maxima of $Ru(bpy)_3^{2+}$ and $Ru(bpy)_2(dtfmbpy)^{2+}$. Interestingly, the excitation band maxima are in surprisingly poor agreement with the MLCT absorptions in room-temperature solution (Figure 4). In the spectra of the bpy and dialkyl-substituted bipyridyl complexes, the longest wavelength excitation maximum is shifted by 3000−4000 cm^{-1} to the red of the MLCT absorption band in the corresponding room-temperature fluid solution absorption spectrum. The dtfmbpy derivative exhibits a smaller red shift ($\sim$900 cm^{-1}). These observations contrast sharply with previous emission studies of platinum(II) bipyridyl complexes in frozen solution, which suggest that the MLCT band in the excitation spectrum typically exhibits a small blue shift from the fluid solution absorption maximum.[46,49] The accumulated data are consistent with a decrease in the average apical Pt···S contact and narrowing of the distribution of conformers in frozen solution, as might be expected for an enthalpically driven, but entropically disfavored apical Pt···S interaction. The comparatively smaller red shift

(67) Klein, A.; van Slageren, J.; Záliš, S. *Eur. J. Inorg. Chem.* **2003**, 1917−1928.
(68) Chan, S.-C.; Chan, M. C. W.; Wang, Y.; Che, C.-M.; Cheung, K.-K.; Zhu, N. *Chem.-Eur. J.* **2001**, *7*, 4180−4190.
(69) Wadas, T. J.; Lachicotte, R. J.; Eisenberg, R. *Inorg. Chem.* **2003**, *42*, 3772−3778.
(70) Dungey, K. E.; Thompson, B. D.; Kane-Magiore, N. A. P.; Wright, L. L. *Inorg. Chem.* **2000**, *39*, 5192−5196.

observed for the dtfmbpy complex is in accord with the view that the Pt···S interactions in room-temperature solutions of this compound are enhanced and that there is a smaller decrease in the average Pt···S contact upon freezing. In support of this interpretation, the Stokes shifts between the room-temperature absorption and 77 K emission maxima (6200−9000 cm^{-1}) are comparatively large, whereas the differences between the 77 K excitation and emission maxima (4800−5900 cm^{-1}) are in excellent agreement with Stokes shifts reported for other platinum(II) diimine complexes that exhibit MLCT emissions (Pt(bpy)$(dmpz)_2$, 6500 cm^{-1}; Pt(3,3′-$(CO_2Me)_2$-bpy)Cl_2, 5500 cm^{-1}).[46,50]

Conclusions

The results presented here reveal an intimate relationship between the molecular and electronic structures of platinum(II) complexes with a dangling nucleophile. We find that the apical Pt···S distances in solid samples of SQP platinum(II) ttcn complexes correlate with the donor properties of the ancillary ligands, suggesting the notion of tuning molecular structure by varying ligand electronic properties. Both π- and σ-donor character decrease positive charge on the metal center and disfavor electrostatic and charge-transfer interactions between the metal and apical sulfur group. Although the precise extent to which these interactions persist in solution is not presently known, their presence significantly impacts the fluid and frozen solution spectroscopy of the bipyridyl complexes reported here. Notably, MLCT states involving the bipyridyl ligand are remarkably stabilized, as expected for sulfur-to-Pt charge-transfer interactions, as well as electron−electron repulsions. The accumulated data are consistent with a distribution of conformers characterized by their different Pt···S distances. Upon freezing, shorter contacts are favored, as expected for enthalpically driven, but entropically unfavorable apical Pt···S bonding. Therefore, these results support the view that a significant population of complexes with short apical Pt···S contacts is present in solution, and fluxional behavior and/or absence of coupling to ^{195}Pt in NMR spectra cannot be taken as evidence to the contrary. Furthermore, it is intriguing to note that the apical interactions are enhanced in solutions of Pt(dtfmbpy)$(ttcn)^{2+}$ as compared to the other complexes, and this result points to the synergistic influence of the dtfmbpy ligand on the energy of the MLCT states of Pt(dtfmbpy)$(ttcn)^{2+}$. The poor donor properties of the dtfmbpy ligand likely increase the acidity of the metal center and enhance apical Pt···S interactions, thereby stabilizing the MLCT states. These results support the corollary that variations in molecular geometry can be used to tune electronic properties of these systems. We believe that a detailed understanding of this delicate interplay between molecular and electronic structures is critical to controlling preorganization and reactivity of these and related systems.

Acknowledgment. Diffraction data for [Pt(dbbpy)(ttcn)]$(PF_6)_2$·CH_3NO_2 and [Pt(dbbpy)(ttcn)]$(PF_6)_2$·$2CH_3CN$·$0.5C_6H_6$ were collected using a SMART 1K diffractometer through the Ohio Crystallographic Consortium, funded by the Ohio Board of Regents 1995 Investment Fund (CAP-075) and located at the University of Toledo Instrumentation Center in Toledo, OH 43606. Diffraction data for [Pt(4,4′-dmbpy)(ttcn)]$(PF_6)_2$·CH_3CN·H_2O, [Pt(5,5′-dmbpy)(ttcn)]$(PF_6)_2$, and [Pt(dtfmbpy)(ttcn)]$(PF_6)_2$·CH_3CN were collected using a SMART6000 diffractometer funded through NSF-MRI grant CHE-0215950. J.A.K.B. thanks Dr. Alan Pinkerton (Department of Chemistry, University of Toledo) for the use of his SMART6000 diffractometer for the data collection of [Pt(bpy)(ttcn)]$(PF_6)_2$. W.B.C. thanks the National Science Foundation (CHE-0134975) for their generous support and the Arnold and Mabel Beckman Foundation for a Young Investigator Award. T.W.G. and W.B.C. thank the University of Cincinnati University Research Council for summer research fellowships. T.W.G. thanks the University of Cincinnati Research Associates and Sigma Xi for their support. In addition, we are grateful to Drs. Koka Jayasimhulu, Elwood Brooks, Ahmed Galal, and Nathan Coker for helpful discussions and technical expertise.

Supporting Information Available: Figures S1 and S2 and crystallographic data in CIF format for all compounds, including [Pt(dbbpy)(ttcn)]$(PF_6)_2$·$2CH_3CN$·$0.5C_6H_6$. This material is available free of charge via the Internet at http://pubs.acs.org.

IC048610D